Analysis of Complex Behaviors on Memristor–Based Bonhöeffer van der Pol Oscillator

Yukinojo Kotani, Yoko Uwate, and Yoshifumi Nishio
Department of Electrical and Electronic Engineering,
Tokushima University
Email: {kotani, uwate, nishio}@ee.tokushima-u.ac.jp

***Abstract*—We propose a memristor–based Bonhöeffer van der Pol oscillator. The three types of the chaotic attractors; one–scroll positive attractor, one–scroll negative attractor, and two–scroll attractor are investigated by replacing the third-power nonlinear resistor with the memristor. In addition, the one parameter bifurcation is obtained by changing the parameter of the memristor. Finally, we do numerical and theoretical analysis to make clear the complex behaviors.**

I. Introduction

Chaos has four properties; nonlinearity, sensitive of initial conditions dependence, boundedness, and nonperiodicity. In the electrical fields, chaos has been investigated on the chaotic systems, and it is applied for network modeling [1-3], security systems [4-6], and complex network of coupled chaotic circuits [7-9]. Many research groups have used a memristor for the chaotic circuits to reveal the complex behaviors, and applied for the technologies of chaos [10-13]. In particular, a Bonhöeffer van der Pol oscillator is one of the chaotic circuits in Fig. 1, and it is developed for network systems [3], [14]. This circuit has the chaotic attractor and the one periodic attractor coexist in Fig. 2.

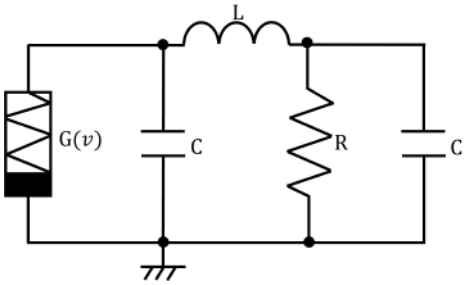

Fig. 1: Bonhöeffer van der Pol oscillator.

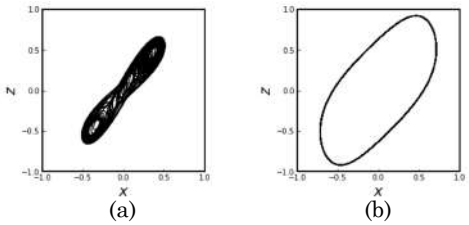

(a) (b)

Fig. 2: Numerical simulation results. (a) Chaotic attractor. (b) Periodic attractor.

A memristor is theoretically introduced by L. O. Chua in 1971 [15]. It is known as the fourth basic circuit element. The conductance (the resistance) of the memoristor depends on the flux (the charge). Many researchers have obtained new chaos in the chaotic circuits by using the memristors [10-13]. However, the memristor–based Bonhöeffer van der Pol oscillator has not been proposed. Therefore, we focus on using the memristor for the Bonhöeffer van der Pol oscillator.

In this study, we propose the memristor–based Bonhöeffer van der Pol oscillator. First, we evaluate the complex behaviors of the numerical simulation results, and corresponds the attactors and the Lyapunov exponents. Second, we investigate the effect of the memristor for the chaotic behaviors to calculate the time series of the flux of the memristor. Third, we investigate the complex behaviors dependence on the memristor changing the one parameter of the memristor. Finally, we analyze the stable and unstable states considering the dependence on the flux of the memristor.

II. Proposed Model

Figure 3(a) shows the schematic model of the flux-controlled third-power memristor, and Fig. 3(b) shows the flux φ – charge q characteristic curve of the memristor [10, 11].

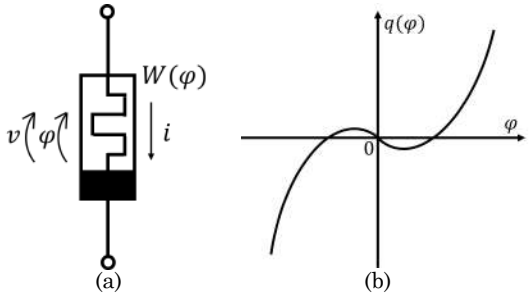

(a) (b)

Fig. 3: Memristor model. (a) Schematic model. (b) φ–q characteristic curve.

The conductance of the memristor $W(\varphi)$ is called memductance. The memristor is characterized by the third-power function $q(\varphi)$, and the memductance $W(\varphi)$ is defined as the gradient of the function $q(\varphi)$.

$$q(\varphi) = -a\varphi + b\varphi^3 \qquad (a, b > 0). \tag{1}$$

$$W(\varphi) = \frac{dq(\varphi)}{d\varphi} = -a + 3b\varphi^2. \tag{2}$$

979-8-3503-7877-1/24/$31.00 ©2024 IEEE

We replace the flux-controlled memristor model of the third-power nonlinear resistor of the Bonhöeffer van der Pol oscillator. Figure 4 shows the memristor–based Bonhöeffer van der Pol oscillator.

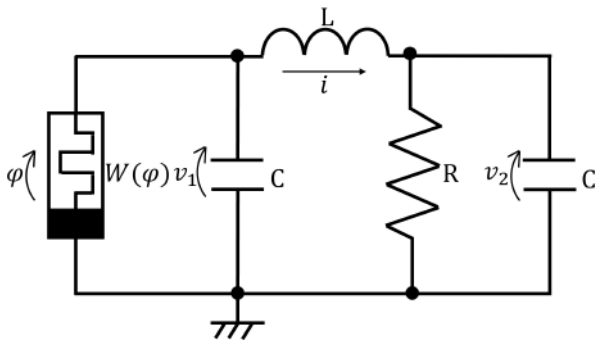

Fig. 4: Memristor–based Bonhöeffer van der Pol oscillator.

The circuit equations are derived as follows from Kirchhoff's laws.

$$\begin{cases} C\dfrac{dv_1}{dt} = -v_1 W(\varphi) - i \\ C\dfrac{dv_2}{dt} = -\dfrac{v_2}{R} + i \\ L\dfrac{di}{dt} = v_1 - v_2 \\ \dfrac{d\varphi}{dt} = v_1. \end{cases} \tag{3}$$

For numerical calculations, the circuit equations in Eq. (3) should be normalized. The variables and parameters are as follow.

$$\begin{aligned} v_1 = \frac{1}{\sqrt{LC}}x, \quad v_2 = \frac{1}{\sqrt{LC}}y, \quad i = \frac{1}{L}z, \quad \varphi = w \\ t = \sqrt{LC}\tau, \quad \alpha = \sqrt{\frac{L}{C}}, \quad \beta = \frac{1}{R}\sqrt{\frac{L}{C}}. \end{aligned} \tag{4}$$

Hence, the normalized circuit equations are given as follows.

$$\begin{cases} \dfrac{dx}{d\tau} = -\alpha W(w)x - z \\ \dfrac{dy}{d\tau} = -\beta y + z \\ \dfrac{dz}{d\tau} = x - y \\ \dfrac{dw}{d\tau} = x. \end{cases} \tag{5}$$

In addition, the $q-\varphi$ characteristic curve of the memristor is also normalized as follows.

$$q(w) = -aw + bw^3 \qquad (a, b > 0). \tag{6}$$

$$W(w) = \frac{dq(w)}{dw} = -a + 3bw^2. \tag{7}$$

By calculating the normalized circuit equations by the Runge–Kutta method, we investigate the complex behaviors of the memristor–based Bonhöeffer van der Pol oscillator. Here, the step size of the Runge–Kutta method $h = 0.01$.

III. Results

A. Chaotic behaviors

We investigate the chaotic state on the several initial conditions (x, y, z, w). The parameters $\alpha = 1.46$, $\beta = 1.25$, $a = 1$, and $b = 1/3$. Figure 5(a) and (b) show the chaotic attractors. In addition, we derive the Poincaré maps to analyze the chaotic state. We define Poincaré section as the region $H \in \{x = 0,\ y > 0\}$. Figure 5(c) shows the chaotic Poincaré maps when the solution orbits pass through the Poincaré section H.

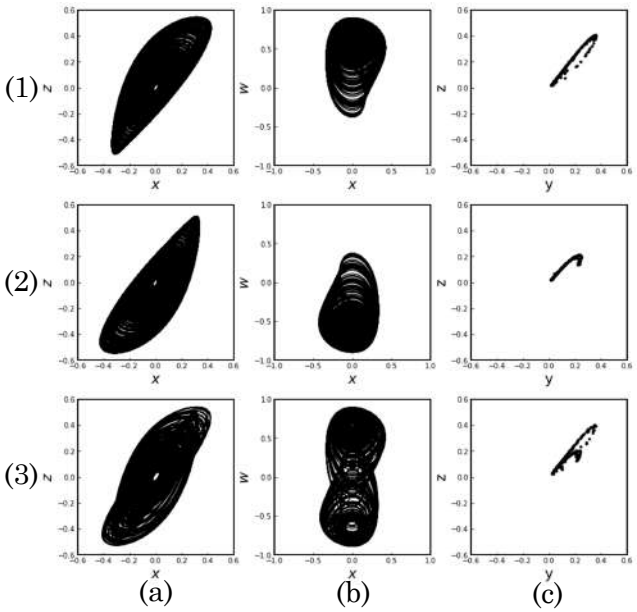

Fig. 5: Numerical simulation results of the chaotic attractors [τ : 14,000, 16,000]. (1) Initial condition (0.001, 0.001, 0, 0). (2) Initial condition (-0.001, -0.001, 0, 0). (3) Initial condition (0.001, 0, 0, 0). (a) Chaotic attractors (x-z). (b) Chaotic attractors (x-w). (c) Poincaré maps (y-z).

On the several initial conditions, we obtain three types of the chaotic attractors; one–scroll positive attractor, one–scroll negative attractor, and two–scroll attractor by replacing the third-power nonlinear resistor with the memristor.

Next, we calculate the Lyapunov exponent, which means averages of divergence. If it is positive and the total of all of them is negative, the attractor represents chaos. The Lyapunov exponents λ_k of each initial condition are listed in Tab. I. Figure 7 shows the time series of λ_k. The index $k = 1, 2, 3, 4$. λ_k is calculated by QR method [10].

TABLE I: Lyapunov exponents of the chaotic attractors.

	Lyapunov exponents			
	λ_1	λ_2	λ_3	λ_4
Case (1)	0.0397	0.000	0.000	-0.3571
Case (2)	0.0397	0.000	0.000	-0.3571
Case (3)	0.0482	0.000	0.000	-0.3320

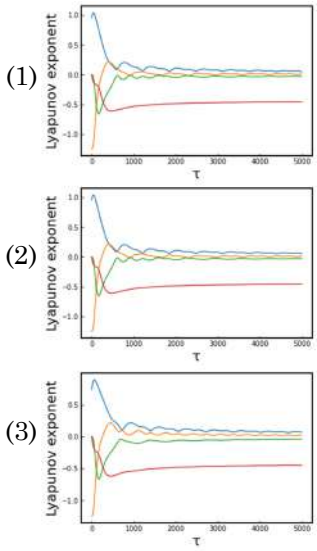

Fig. 6: Numerical simulation results of the time series of the Lyapunov exponent. (1) Initial condition (0.001, 0.001, 0, 0). (2) Initial condition (-0.001, -0.001, 0, 0). (3) Initial condition (0.001, 0, 0, 0).

All the Lyapunov exponents λ_1 have positive values in Tab. I. The attractors in Fig. 5 represent chaos by calculating the normalized circuit equations and the Lyapunov exponents.

Moreover, we focus on the memristor behaviors, and research the effect for the chaotic state. Figure 7(a) shows the time series of x, and Fig. 7(b) shows the time series of w.

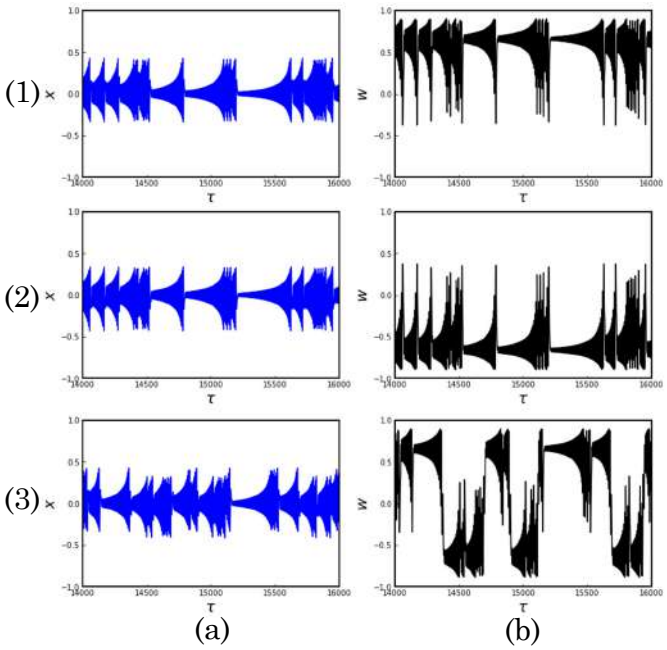

Fig. 7: Numerical simulation results of the time series [τ : 14,000, 16,000]. (1) Initial condition (0.001, 0.001, 0, 0). (2) Initial condition (-0.001, -0.001, 0, 0). (3) Initial condition (0.001, 0, 0, 0). (a) Time series of x. (b) Time series of w.

In Fig. 7(a), x oscillates in the region $-0.50 \leq a \leq 0.50$ on all the initial conditions. On the other hand, in Fig. 7(b), the time series of w when the case (1) shows that w oscillates in the positive region. Similarly, w also oscillates in the negative region when the case (2). When the case (3), w oscillates in the positive and negative regions. Comparing the chaotic attractor and the time series of w, the types of the chaotic attractors depends on the changes of the variable of the memristor w. Therefore, three types of the chaotic state are observed by changing the initial conditions and the behaviors of w.

B. Complex behavior dependence on memristor

We investigate the complex behaviors dependence on the memristor by changing the one parameter of the memristor a. We fix the initial condition (0, 0.001, 0, 0) and the parameters $\alpha = 1.46$, $\beta = 1.25$, $b = 1/3$. The periodic attractors are shown in Fig. 8 (a) and (b). Figure 8(c) shows the Poincaré maps. We also calculate the Lyapunov exponents λ_k of each initial condition in Tab. II.

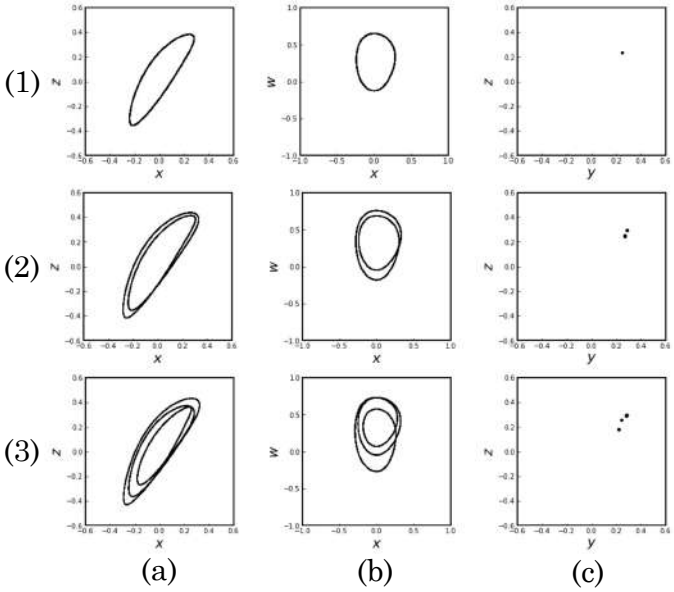

Fig. 8: Numerical simulation results of the periodic attractors [τ : 14,000, 16,000]. (1) $a = 0.95$. (2) $a = 0.97$. (3) $a = 0.96$. (a) Periodic attractors (x-z). (b) Periodic attractors (x-w). (c) Poincaré maps (y-z).

TABLE II: Lyapunov exponents of the periodic attractors.

	Lyapunov exponents			
	λ_1	λ_2	λ_3	λ_4
Case (1)	0.000	0.000	-0.0267	-0.0268
Case (2)	0.000	0.000	-0.0345	-0.0347
Case (3)	0.000	0.000	-0.0015	-0.0807

Comparing the numerical simulation results of the periodic attractors and the Lyapunov exponents, we obtain the one periodic, the two periodic, and the three periodic attractors by changing the one parameter of the memristor a. In addition, Fig. 9 shows the one parameter bifurcation diagram.

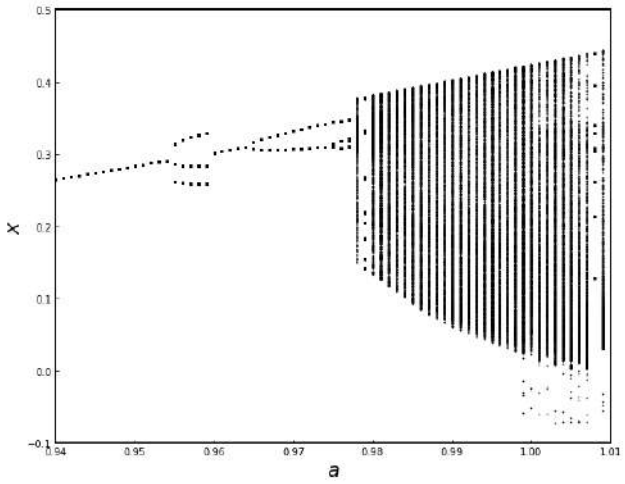

Fig. 9: One parameter bifurcation diagram. Initial conditions (0, 0.001, 0, 0).

In Fig. 9, the periodic attractors are observed in the region $0.94 \leq a \leq 0.987$. On the other hand, the chaotic attractors are also observed in the region of $0.988 \leq a \leq 1.01$. Therefore, the one parameter bifurcation diagram is obtained.

C. Stable analysis

We investigate the stable state of the memristor–based Bonhöeffer van der Pol oscillator. The equilibrium points are obtained by letting $dx/d\tau = dy/d\tau = dz/d\tau = dw/d\tau = 0$. The equilibrium state of Eq. (5) is given by set $A = \{(x, y, z, w)|x = y = z = 0, w = p\}$. Here, p is constant. The Jacobian matrix $\mathbf{J}$ at this equilibrium set is given by Eq. (8).

$$\mathbf{J} = \begin{pmatrix} -\alpha W(p) & 0 & -1 & 0 \\ 0 & -\beta & 1 & 0 \\ 1 & -1 & 0 & 0 \\ 1 & 0 & 0 & 0 \end{pmatrix}. \tag{8}$$

Here, $W(p) = -a + 3bp^2$. The characteristic equation is obtained from the determinant in Eq. (9).

$$\mathbf{det}(\mathbf{J} - \rho\mathbf{E}) = 0. \tag{9}$$

Here, ρ is the eigenvalues, and $\mathbf{E}$ is an identity matrix. By calculating the determinant in Eq. (9), we get the characteristic equation of the memristor–based Bonhöeffer van der Pol oscillator.

$$(a_0{\rho_k}^3 + a_1{\rho_k}^2 + a_2\rho_k + a_3)\rho_k = 0. \tag{10}$$

The coefficients $a_0 = 1$, $a_1 = \alpha W(p) + \beta$, $a_2 = \alpha\beta W(p) + 2$, $a_3 = \alpha W(p) + \beta$. From Eq. (10), the Jacobian matrix $\mathbf{J}$ has a zero eigenvalue ρ_1 and three nonzero eigenvalues ρ_2, ρ_3, ρ_4. The stable criterion of Eq. (10) is derived from the Hurwitz criterion. a_0 is positive, so Eq. (10) satisfies the following criterion.

1) The coefficients a_1, a_2 and a_3 are positive.
2) All the Hurwitz matrices $\mathbf{D_1}$, $\mathbf{D_2}$, and $\mathbf{D_3}$ are positive.

Therefore, the Hurwitz matrices $\mathbf{D_1}$, $\mathbf{D_2}$, and $\mathbf{D_3}$ are as follows.

$$\begin{aligned} \mathbf{D_1} &= a_1 > 0 \\ \mathbf{D_2} &= \begin{vmatrix} a_1 & a_2 \\ 1 & a_3 \end{vmatrix} = a_1a_3 - a_2 > 0 \\ \mathbf{D_3} &= \begin{vmatrix} a_1 & a_2 & 0 \\ 1 & a_3 & 0 \\ 0 & a_1 & a_3 \end{vmatrix} = a_3(a_1a_2 - a_3) > 0 \end{aligned}. \tag{11}$$

We set $\alpha = 1.46$, $\beta = 1.25$, $a = 1$, $b = 1/3$. Therefore, the stable criterion is obtained as follows.

$$|p| > 0.6724. \tag{12}$$

In other word, the unstable criterion is shown in Eq. (13).

$$|p| < 0.6724. \tag{13}$$

Table III shows the list of the three eigenvalues of Eq. (10).

TABLE III: The three nonzero eigenvalues ρ_k.

$\lvert p\rvert$	**Eigenvalues** ρ_k		
	ρ_2	ρ_3	ρ_4
0	0.5625	$-0.1763 - j\sqrt{0.5850}$	$-0.1763 + j\sqrt{0.5850}$
0.6	-0.3703	$0.02735 - j\sqrt{0.9228}$	$0.02735 + j\sqrt{0.9228}$
0.66	-0.4370	$0.0055 - j\sqrt{0.9873}$	$0.0055 + j\sqrt{0.9873}$
0.6724	-0.4501	$-j\sqrt{1.0001}$	$j\sqrt{1.0001}$
0.68	-0.4580	$-0.0035 - j\sqrt{1.0078}$	$-0.0035 + j\sqrt{1.0078}$
0.7	-0.4784	$-0.0135 - j\sqrt{1.0277}$	$-0.0135 + j\sqrt{1.0277}$

j is the imaginary unit. In Tab. III, all the real parts of ρ_k are negative in the region $0.6724 < |p| \leq 0.7$, which indicates that the equilibrium set A is stable. On the other hand, at least ρ_k has the positive real parts in the region $0 \leq |p| < 0.6724$, which indicates that the equilibrium set A is unstable. Therefore, the stable criterion depends on the initial condition of the memristor.

CONCLUSIONS

We proposed the memristor–based Bonhöeffer van der Pol oscillator. First, we obtained the three types of the chaotic attractors; one–scroll positive attractor, one–scroll negative attractor, and two–scroll attractor by replacing the third-power nonlinear resistor with the memristor. Second, the shape of the chaotic attractors is characterized by the flux of the memristor. Third, the periodic attractor; the one periodic, the two periodic, and three periodic attractor are obtained, and the one parameter bifurcation diagram occurs. Finally, the stable analysis indicates that the stable and unstable criterion depends on the initial condition of the memristor.

In the future, we would like to design the flux-controlled third-power memristor model, and compare the results of the numerical simulation results and those of the circuit experiments to provide the fundamental evidences. In addition, we would like to expand the scale of the circuit model, such as the coupled memristor–based Bonohöeffer van der Pol oscillator, and investigate the chaos synchronization to develop the applications using the circuit network systems.

REFERENCES

[1] C. Xiu, J. Hou, Y. Zang, G. Xu, and C. Liu, "Synchronous Control of Hysteretic Creep Chaotic Neural Network," IEEE Access, vol. 4, no. 2, pp. 8617–8624, Apr. 2017.

[2] C. Pan, Q. Hong, and X. Wang, "A Novel Memristive Chaotic Neuron Circuit and Its Application in Chaotic Neural Networks for Associative Memory," IEEE Trans. Comput. Aided Des. Integr. Circuits Syst., vol. 40, no. 3, pp. 521–532, Mar. 2021.

[3] K. Yasufuku, Y. Uwate, and Y. Nishio, "A Study of Changes in Prediction Performance Influenced by Attractor State in Oscillator Reservoir Computing," Proc. of Int. Conf. ISOCC'23, pp. 259–260, Oct. 2023.

[4] K. Benkouider, T. Bouden, A. Sambas, M. A. Mohamed, I. M. Sulaiman, M. Mamat, and M. A. H. Ibrahim, "Dynamics, Control and Secure Transmission Electronic Circuit Implementation of a New 3D Chaotic System in Comparison With 50 Reported Systems," IEEE Access, vol. 9, pp. 152150–152168, Nov. 2021.

[5] H. S. Park, and S. K. Hong, "Encryption Device Based on Wave-Chaos for Enhanced Physical Security of Wireless Wave Transmission," IEEE Access, vol. 11, pp. 102917–102925, Sep. 2023.

[6] W. E. H. Youssef, A. Abdelli, F. Kharroubi, F. Dridi, L. Khriji, R. Ahshan, M. Machhout, S. H. Nengroo, and S. Lee, "A Secure Chaos-Based Lightweight Cryptosystem for the Internet of Things," IEEE Access, vol. 11, pp. 123279–123294, Oct. 2023.

[7] M. Chen, "Chaos Synchronization in Complex Networks," IEEE Trans. on Circuits and Syst. I:Regular Papers, vol. 55, Issue pp. 1335–1346, Jun. 2008.

[8] Y. Nishio, and Y. Uwate, "Clusteling Methods Using Synchronization of Chaotic Circuit Networks," Proc. of Int. Conf. ISOCC'19, pp. 152–153, Oct. 2019.

[9] Y. Uwate, Y. Nishio, and T. Ott, "Synchronization of Chaotic Circuits with Stochastically-Coupled Network Topology," Int. J. Bifurcation Chaos, vol. 31, no. 1, pp. 2150015_1–7, Jan. 2021.

[10] B. Bao, and Z. Ma, "A Simple Memristor Chaotic Circuit with Complex Dynamics," Int. J. Bifurcation Chaos, vol. 21, no. 9, pp. 2629–2645, Sep. 2011.

[11] K. Dong, K. Xu, Y. Zhou, C. Zuo, L. Wang, C. Zhang, F. Jin, J. Song, W. Mo, and Y. Hui, "A Memristor-Based Chaotic Oscillator for Weak Signal Detection and Its Circuitry Realization," Nonlinear Dyn. vol. 109, pp. 2129–2141, Jun. 2022.

[12] S. Wen, Y. Shen, Z. Zeng and Y. Cai, "Chaos Analysis and Control in a Chaotic Circuit with a PWL Memristor," Proc. of Int. Conf. on ICIST'11, pp. 1030–1033, Mar. 2011.

[13] G. Wang, M. Cui, B. Cai, X. Wang, and T. Hu, "A Chaotic Oscillator Based on HP Memristor Model," Hindawi Publishing Corporation Mathematical Problems in Engineering, vol. 2015, pp. 1–12, Oct. 2015.

[14] K. Ueta, Y. Uwate, and Y. Nishio, "Analysis of Frustration by Coupled Ring and Star of BVP-VDP Oscillator," Proc. of IEEE Workshop NCN'17, pp. 72-75, Dec. 2017.

[15] L . O. Chua, "Memristor–The Missing Circuit Element," IEEE Trans. on Circuit Theory, vol. CT-18, no. 5, Sep. 1971.